Available online at www.sciencedirect.com

ScienceDirect

Russian Geology and Geophysics 54 (2013) 1205–1218

RUSSIAN GEOLOGY AND GEOPHYSICS

www.elsevier.com/locate/rgg

Synmetamorphic granitoids (~490 Ma) as accretion indicators in the evolution of the Ol'khon terrane (*western Cisbaikalia*)

T.V. Donskaya [a,*], D.P. Gladkochub [a], V.S. Fedorovsky [b], A.M. Mazukabzov [a], M. Cho [c], W. Cheong [c], J. Kim [d]

[a] *Institute of the Earth's Crust, Siberian Branch of the Russian Academy of Sciences, ul. Lermontova 128, Irkutsk, 664033, Russia*
[b] *Geological Institute, Russian Academy of Sciences, Pyzhevskii per. 7, 119017, Moscow, Russia*
[c] *School of Earth and Environmental Sciences, Seoul National University, Seoul 151-747, Korea*
[d] *Division of Earth and Environmental Sciences, Korea Basic Science Institute, Ochang 363-883, Korea*

Received 26 March 2013; received in revised form 16 May 3013; accepted 23 May 2013

Abstract

We present geological, structural, and geochemical data on synmetamorphic granitoids from the Tutai and South Ol'khon plutons of the Ol'khon terrane (Central Asian Fold Belt) with an estimation of the U–Pb zircon age of the Tutai granites. The structural and petrological data suggest the synfolding and synmetamorphic origin of the granitoids. The U–Pb zircon age of the Tutai granites (488.6 ± 8.0 Ma) almost coincides with the previously estimated age of quartz syenites from the South Ol'khon pluton (495 ± 6 Ma). The plutons occupy the same position in the regional structure. The granitoids underwent final deformations and metamorphism at 464 ± 11 Ma. The Tutai pluton consists of moderately potassic granites, whereas the South Ol'khon pluton is made up of quartz syenites and granites. The geochemical characteristics of the granites from both plutons (low Y and Yb contents, fractionated REE patterns) indicate their formation under conditions of garnet crystallization in deep crustal restite. The higher Y and Yb contents of the South Ol'khon quartz syenites as compared with those of the granites suggest the lack of equilibrium between the quartz syenite magmas and garnet parageneses during their formation or evolution. The Tutai and South Ol'khon granites were derived from quartz-feldspar crustal rocks, whereas the South Ol'khon quartz syenites might have originated from a mixed (crust-mantle) source. It is presumed that the granitoids formed within accretion-thickened crust. Early accretion, which has been first identified in the region, affected not only the Pribrezhnaya zone (the zone of the Tutai and South Ol'khon plutons) but also the entire Anga–Satyurty megazone of the Ol'khon terrane. The accretion ended with the convergence and oblique collision of the Ol'khon terrane and Siberian continent, when strike-slip tectonics became ubiquitous.
© 2013, V.S. Sobolev IGM, Siberian Branch of the RAS. Published by Elsevier B.V. All rights reserved.

Keywords: granites; quartz syenites; U–Pb geochronology; geochemistry; accretion; collision; Early Paleozoic; Ol'khon terrane; Central Asian Fold Belt

Introduction

It is a complicated, multistage problem to decipher the scenarios of the geodynamic evolution of metamorphic terranes whose rocks have undergone repeated deformations accompanied by pulsed igneous activity. Particular difficulties arise in the case of a narrow time interval including metamorphic and igneous events and overlapping estimated ages of rocks in different segments of strongly dislocated terranes. One of such structures is the Ol'khon metamorphic terrane, localized in the northern Central Asian Fold Belt. The Ol'khon terrane, like similar structures of the Baikal collisional metamorphic belt (Derba, Kitoikin, Slyudyanka, and Barguzin terranes), was formed predominantly in the Early Paleozoic by the accretion and collision of different parts of Neoproterozoic–Early Paleozoic island arcs and backarc basins as well as fragments of Precambrian microcontinents with respect to one another and their accretion to the Siberian craton (Dobretsov and Buslov, 2007; Donskaya et al., 2000; Gladkochub et al., 2008b; Metelkin et al., 2012; Nozhkin et al., 2005; Rytsk et al., 2009; Salnikova et al., 1998). The belt extends for >1000 km along the southern cratonic boundary (Fig. 1*a*).

All the reliably dated (U–Pb zircon method) metamorphic and igneous events within the Ol'khon terrane took place from 510 to 460 Ma (Bibikova et al., 1990; Fedorovsky et al., 2005, 2010; Gladkochub et al., 2008b; Sklyarov et al., 2009; Vladimirov et al., 2008; Volkova et al., 2010). The metamor-

* Corresponding author.
E-mail address: tanlen@crust.irk.ru (T.V. Donskaya)

1068-7971/$ - see front matter © 2013, V.S. Sobolev IGM, Siberian Branch of the RAS. Published by Elsevier B.V. All rights reserved.
http://dx.doi.org/10.1016/j.rgg.2013.09.006

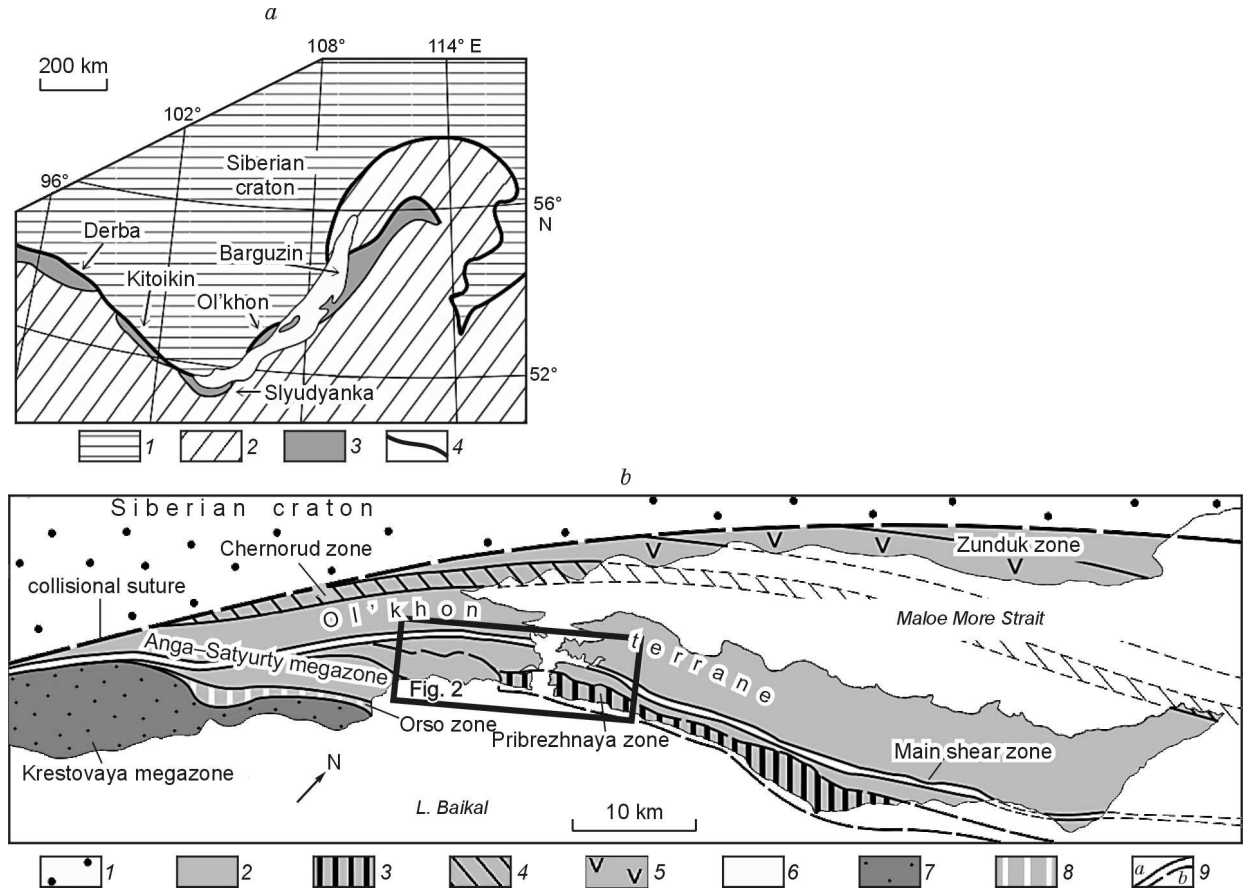

Fig. 1. Location of metamorphic terranes in the southern framing of the Siberian craton (Baikal collisional metamorphic belt) (Donskaya et al., 2000; Nozhkin et al., 2005; Rytsk et al., 2009) (*a*) and location of the main structures of the Ol'khon region with the position of the Pribrezhnaya zone (*b*). *a*: *1*, Siberian craton; *2*, Central Asian Fold Belt; *3*, metamorphic terranes of the Baikal collisional belt; *4*, main faults; *b*: *1*, Siberian craton; *2–8*, Ol'khon terrane: *2*, Anga–Satyurty megazone; *3–6*, some zones within the Anga–Satyurty megazone: *3*, Pribrezhnaya zone; *4*, Chernorud zone; *5*, Zunduk zone; *6*, Main shear zone; *7*, Krestovaya megazone; *8*, Orso zone; *9*, strike-slip sutures (*a*) and boundaries of the Pribrezhnaya zone (*b*).

phic events and episodes of igneous activity often yield close estimated ages.

We consider the results of geochronological and geochemical studies of the synmetamorphic granitoids making up plutons in the eastern Ol'khon metamorphic terrane. These data, combined with geological and tectonic data on the study area and the entire region, provide a better understanding of the structure of the Ol'khon terrane and a scenario of its geodynamic evolution.

Geologic and tectonic summary of the Ol'khon terrane

The Ol'khon metamorphic terrane, consisting of the continental part and Ol'khon Island, is located along the western shore of Lake Baikal (Fig. 1*b*). This terrane is sometimes assigned to a larger tectonic unit, which spans the southern and eastern shores of Lake Baikal (Makrygina et al., 2007; Volkova and Sklyarov, 2007). The Ol'khon terrane consists of sedimentary, volcanic, and plutonic rocks, most of which are affected by regional metamorphism, varying from the low-grade amphibolitic facies to the granulitic facies (Fedorovsky et al., 2005; Rosen and Fedorovskii, 2001). The terrane rocks make up several complexes, which formed in Neoproterozoic–Early Paleozoic island-arc-system, backarc-system, and, probably, microcontinental settings and were tectonically compressed in a collisional collage (Fedorovsky et al., 2005; Gladkochub et al., 2008a, 2010; Makrygina et al., 2007; Mazukabzov et al., 2010; Zorin et al., 2009).

The Ol'khon terrane is separated from the Siberian craton by a collisional suture (Fig. 1*b*) (Fedorovskii et al., 1995; Fedorovsky et al., 2005; Sukhorukov et al., 2005). The terrane now consists of groups of NE-striking tectonic sheets separated by blastomylonite sutures. The internal structure of the sheets has a great variety of forms, produced by synmetamorphic deformations. Detailed mapping and structural analysis showed that the general tectonic style of the region is associated with strike-slip tectonics, preceded by older synmetamorphic deformations of the sheet and domal types (Fedorovskii et al., 1995; Fedorovsky et al., 2010).

The Ol'khon terrane comprises several principal regional units (megazones, regional zones), which differ in the compositions of metamorphic and igneous rocks, internal structure, geodynamic settings, and other features (Anga–Satyurty and

Krestovaya megazones, Orso zone) (Fig. 1*b*). The Anga–Satyurty megazone occupies about half the study region. Its internal structure is a collage of numerous long, narrow displacement sheets, which consist of gneiss-migmatite rocks (garnet-biotite gneisses and migmatites, granite-gneisses) or "variegated" metamorphic rocks (amphibolites, quartzites, marbles and marble mélanges, calciphyres, mafic gneisses, metagabbro, and metaultramafic rocks), with absent felsic gneisses and migmatites. Both types of sheets are rich in synmetamorphic granite bodies. The Main shear zone of the region occupies a special place in the Anga–Satyurty megazone. This narrow zone, traced for ~120 km, contains numerous small ultramafic bodies (actually, it is an ophiolite suture). It truncates all the other components of the Anga–Satyurty megazone at oblique angles and divides the constituent sheets into two large groups. A considerable extent of the Anga–Satyurty megazone adjoins the collisional suture of the terrane–continent system. Granulite-facies rocks are localized within the Chernorud zone (component of the Anga–Satyurty megazone). These rocks extend as a narrow strip toward the northwestern shore of the Maloe More Strait through islets to Cape Khoboi on the northern tip of Ol'khon Island, behind which they are concealed by the Baikal waters. Along the northeastern (Zunduk zone) and southwestern (Krestovaya megazone) flanks of the collisional suture, no granulites are observed but amphibolite-facies rocks are present.

The Krestovaya megazone occupies the southwestern Ol'khon terrane. This megazone consists of "variegated" metamorphic rocks (epidote-amphibolite–amphibolite facies) and contains large gabbro plutons (Birkhin, Krestovaya, Bugul'deika, and others), which make up more than half its area, and the well-known Tazheran syenite pluton. Structurally, the Krestovaya megazone is composed of several displacement sheets. Numerous large folded sigmoids therein reflect the dramatic rheologic inhomogeneity of the sheared medium.

The Orso zone occupies a special position in the terrane structure. This small (1×25 km) displacement sheet, bounded in the northwest by an ophiolite suture, is made up of garnet-biotite microgneisses and amphibolites. As the collisional suture is approached, the Orso zone, located between the Anga–Satyurty and Krestovaya megazones, wedges out, and the last two megazones are separated by the Main shear zone.

A review of geochronological data on the rocks of different zones of the Ol'khon terrane is given in (Fedorovsky et al., 2005, 2010; Vladimirov et al., 2011). Let us single out the key age estimates. Granulite-facies metamorphism in the Chernorud zone of the Anga–Satyurty megazone is dated at 507 ± 8 to 485 ± 5 Ma (Bibikova et al., 1990; Gladkochub et al., 2008a,b). Age estimates within the same range were obtained for gabbro from the Birkhin pluton of the Krestovaya megazone (499 Ma, data of A.B. Kotov (Fedorovsky et al., 2010)) and for the quartz syenites of the Anga–Satyurty megazone from southern Ol'khon Island (495 ± 6 Ma (Gladkochub et al., 2008b)). Igneous and metamorphic rocks with an age of 458–475 Ma are widespread within the Anga–Satyurty and Krestovaya megazones (Fedorovsky et al., 2010; Sklyarov et al., 2009; Vladimirov et al., 2008).

Geologic structure of the eastern Ol'khon terrane

The eastern Ol'khon terrane spans the areas adjoining the Ol'khonskie Vorota Strait (which separates the Ol'khon area and Ol'khon Island) from the direction of Lake Baikal. Detailed mapping of this area shows a very complicated, strained structure of a collisional collage (Fig. 2). Numerous displacement sheets make up seven zones. Three of them (Central, Tutai, and Holboo Nuur) are composed of gneiss-migmatite rocks (garnet-biotite gneisses, migmatites and granite-gneisses, amphibole gneisses, amphibolites, and synmetamorphic granites). The Main shear zone (ophiolite suture), Nutgei zone, and Orgoita–Zmeinaya Creek zone are located between these units. The Nutgei and Orgoita–Zmeinaya Creek zones consist of "variegated" metamorphic rocks (amphibolites, quartzites, marbles, calciphyres, and marble mélanges) as well as synmetamorphic granites, gabbro, and ultramafic rocks. The contact between the Tutai and Orgoita–Zmeinaya Creek zones has an unusual appearance: Alternating fragments of both zones extend for several kilometers in a wide strip resembling a megamélange belt (Fig. 2). The seventh, Pribrezhnaya, zone is located farther northeast, between the Tutai zone and the tectonic-mélange belt. Its matrix is a complicated interlacing of many short and long displacement sheets, which consist of both gneiss-migmatite and "variegated" rocks. Apparently, it is the continuation of the above-mentioned megamélange belt. Another interesting feature of the Pribrezhnaya zone is the presence of the tectonized granitoid plutons considered in this paper only within its boundaries.

Small isoclinal folds with rounded curves (F_1) are the oldest structural elements observed in the Ol'khon area of the Pribrezhnaya zone. They resemble intrafolial rootless folds with increasing deformation (Turner and Weiss, 1963). Intrafolial folds are observed only in amphibole gneisses. The thin metamorphic banding in these rocks is due to metamorphic differentiation, manifested in leucocratic bands enriched in plagioclase with minor biotite and amphibole-dominated mesocratic rocks. This banding might correspond to vestiges of lamination, which was enhanced by metamorphism. The garnet-biotite gneisses in the Pribrezhnaya zone are characterized by nonuniform migmatization with alternating very thick and very thin banding. These rocks show schistosity, which is brought out by the biotite orientation. The schistosity is paralleled by migmatite veinlets, which form migmatite banding. These structural elements reflect the second deformation stage and the formation of mesoscale folds with gently sloping axial surfaces (F_2). First-generation folds combine with second-stage migmatite banding and schistosity to form third-generation folds (F_3). This event results in macro- to mesoscale folding. Gneiss outcrops show compressed to open folding with an amplitude of up to 1.5 m. The limbs of these folds are often complicated by duplex structures, which are reconstructed from S-shaped foliation and banding. The next

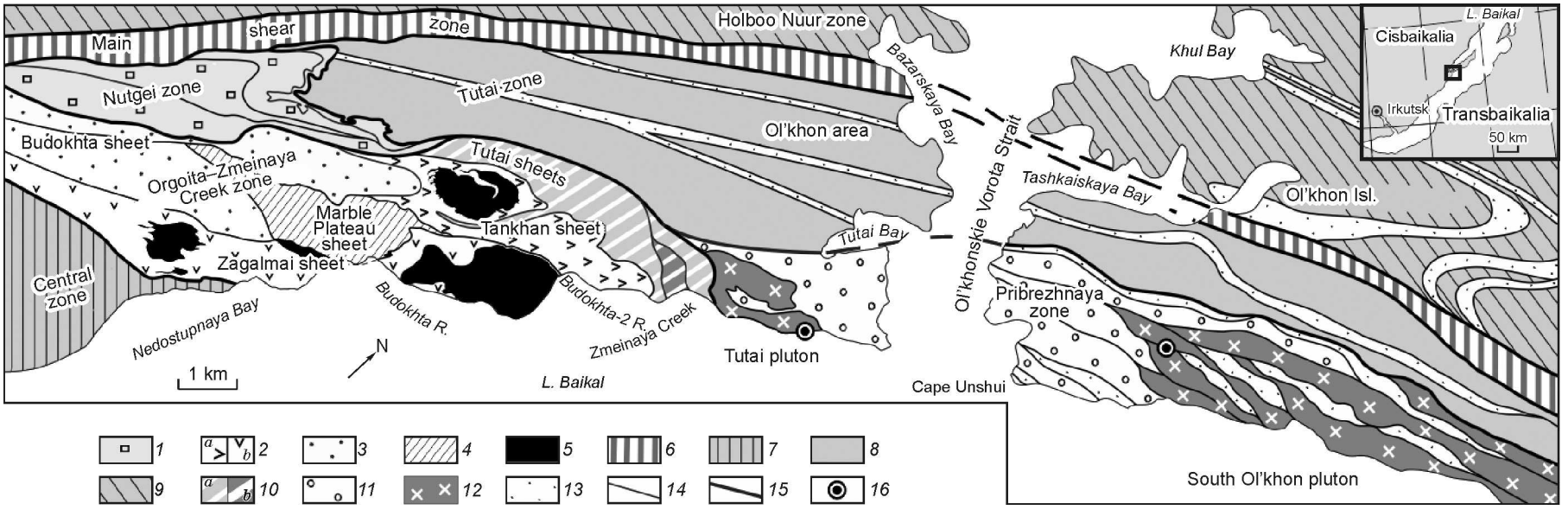

Fig. 2. Tectonic sketch map of the northeastern Ol'khon area (Fedorovskii et al., 2011) and part of Ol'khon Island. *1*, Nutgei zone (amphibolites, quartzites, marbles, marble mélanges, and, sometimes, ultramafic rocks); *2–5*, Orgoita–Zmeinaya Creek zone: *2*, Tankhan (*a*) and Zagalmai (*b*) sheets (quartzites, amphibolites, marbles, metagabbro, and, rarely, ultramafic rocks); *3*, Budokhta sheet (amphibolites, marbles, marble mélanges, and quartzites); *4*, Marble Plateau (marbles and marble mélanges); *5*, blocked metagabbro plutons affected by rolling; *6*, Main shear zone (amphibolites, quartzites, marbles and marble mélanges, ultramafic rocks, synmetamorphic granites); *7–9*, displacement sheets of biotitic and garnet-biotite gneisses and migmatites, granite-gneisses, and synmetamorphic granites: *7*, Central zone; *8*, Tutai zone; *9*, Holboo Nuur zone; *10*, tectonic mingling of fragments of the Tutai zone (*a*) and the Orgoita–Zmeinaya Creek zone (*b*); *11*, *12*, Pribrezhnaya zone: *11*, gneisses, migmatites, granite-gneisses, amphibolites, synmetamorphic granites; *12*, granites and quartz syenites of the Tutai and South Ol'khon plutons; *13*, sutures (amphibolites, marbles, and marble mélanges) in the Pribrezhnaya, Tutai, and Holboo Nuur zones; *14*, tectonic boundaries between the displacement sheets; *15*, tectonic boundaries between the zones; *16*, sampling sites for the geochronological studies.

deformation stage (F_4) is marked by the formation of steeply dipping hinge folds of different scales, which are well reconstructed in garnet-biotite gneisses near granite intrusions. Vertically dipping pegmatite veins of northwestern strike (up to 5 m thick) intrude all the rock complexes of the Pribrezhnaya zone, including the granitoid plutons.

Geological, structural, and petrographical descriptions of the study localities

The tectonized granites of the Tutai pluton in the Ol'khon area of the Pribrezhnaya zone were selected as the main subject of study (Fig. 2). The quartz syenites and granites of the South Ol'khon pluton, which occupy a similar geologic position in the Ol'khon area of the Pribrezhnaya zone, were studied in detail before (Gladkochub et al., 2008b). Their brief description and chemical compositions are also given in this paper for comparison with the Tutai granites.

The Tutai pluton occupies a small area (~2.5 km^2) between Tutai Bay in the Ol'khonskie Vorota Strait and the Zmeinaya Creek, which faces Lake Baikal (Fig. 2). The pluton is elongated for 2.5 km to the northeast and reaches a width of 1 km.

It was presumed before (Kuklei, 1988) that this intrusion, which makes up the Shara Nuur granite-gneiss swell, formed during gneiss granitization, i.e., in situ. However, our observations contradict this hypothesis. The relationships between the Tutai granites and host garnet-biotite gneisses of the Pribrezhnaya zone were observed in the hard rocks of the Baikal-facing slope. Distinct cutting contacts are observed here, but the contacting rocks show no exo- or endocontact alterations, suggesting the isothermal state of the granites and host rocks during the intrusion. The contact character and host-rock xenoliths in the pluton suggest that the granites make up an allochthonous intrusion. It is seen from the outcrops that the migmatized gneisses were intruded by the apophyses extending from the granitoid pluton and then involved in mesoscale folding (F_3) and foliation. Such relationships are well-defined in the littoral outcrops near the mouth of the Zmeinaya Creek. We presume that the Tutai granites intruded during the second deformation stage (F_2), because the granite apophyses are concordant to the migmatite banding and foliation.

The central part of the Tutai pluton is dominated by medium- to coarse-grained massive granites, and its edges are partly gneissose. The main minerals in the granites are quartz, plagioclase, and K-feldspar. The minor minerals are biotite and, sometimes, hornblende. The accessory minerals are titanite, apatite, zircon, and the ore mineral. The rocks show partial shearing, which leads to plagioclase sericitization and the development of secondary muscovite.

The South Ol'khon granite–quartz syenite pluton, which is 1.0–1.5 km wide, extends to the northeast for ~30 km along the rocky shore of Ol'khon Island (Fig. 2). The structural position of the granites and quartz syenites in this pluton is similar to that of the Tutai granites. The rocks of the pluton intrude garnet-biotite gneisses, affected by early deformations, and are involved in later deformations.

The pluton consists of medium-grained quartz syenites and granites, which are often gneissose. The main minerals in the quartz syenites are K-feldspar, plagioclase, quartz, and hornblende. The minor mineral is biotite, and the accessory minerals are apatite, titanite, and zircon. The secondary mineral is epidote. The granites consist of quartz, plagioclase, K-feldspar, hornblende, and biotite. The accessory minerals in the granites are titanite, zircon, apatite, ore mineral; also, secondary muscovite is observed.

The U–Pb zircon age of quartz syenite from the South Ol'khon pluton is 495 ± 6 Ma (Gladkochub et al., 2008b). The $\varepsilon_{Nd}(T)$ value for quartz syenite is estimated at –0.3, and the $^{87}Sr/^{86}Sr$ ratio, at 0.7043 (Gladkochub et al., 2008b).

Methods

Analytical methods for studying the South Ol'khon quartz syenites and granites are given in (Gladkochub et al., 2008b). The major- petrogenic oxides, trace-, and rare-earth element contents of the Tutai granites were determined, and their age was estimated by the U–Pb zircon method. Sampling sites for the geochronological studies are shown in Fig. 2.

The major-element contents were determined by silicate analysis at the Institute of the Earth's Crust (analysts G.V. Bondareva and M.M. Samoilenko). The trace and rare-earth elements were determined by ICP-MS at the Center of Collective Use of the Irkutsk Scientific Center on a VG PlasmaQuad PQ 2 mass spectrometer (VG Elemental, England) (analyst S.V. Panteeva) using the technique of Garbe-Schönberg (1993). The spectrometer was calibrated against the international standards G-2, GSP-2, and JG-2. Chemical digestion of the samples for ICP-MS was conducted by alloying with lithium metaborate using the technique of Panteeva et al. (2003) to achieve complete dissolution of all the minerals. The ICP-MS determination error for the trace and rare-earth elements is no more than 5%.

Some zircon grains from the Tutai granite (sample 1015) were dated by the U–Pb method on a SHRIMP II microprobe at the Korean Basic Science Institute. Cathodoluminescence images of zircon were obtained under a JEOL 6610LV SEM in the cathodoluminescence mode. The U–Pb ratios were measured on a SHRIMP II by the technique described in (Williams, 1998). The intensity of the primary beam of negative molecular oxygen ions was 3–4 nA, and the spot diameter was 20 μm. The measured $^{206}Pb/^{238}U$ ratios were calibrated against the isotope ratio ascribed to 1099 Ma zircon FC1 (Paces and Miller, 1993). The U and Th contents were calculated with respect to zircon SL13 (238 ppm U). The results were processed in the SQUID 2.50 software (Ludwig, 2008), and concordia diagrams were plotted in the Isoplot 3.71 software (Ludwig, 2009). The mean weighted ages were calculated using the $^{206}Pb^*/^{238}U$ ratio, corrected for ^{207}Pb with excluded unsuitable values in the statistical *t*-test.

Petrogeochemical characteristics of the granitoids

In the Tutai granites, SiO_2 = 68.9–71.3 wt.% and (Na_2O + K_2O) = 8.02–8.65 wt.% at $Na_2O > K_2O$ (Na_2O/K_2O = 1.05–1.85). The studied rocks plot as granite on the diagram ($Na_2O + K_2O$)–SiO_2 (Middlemost, 1985) (Fig. 3). Except one sample, all the analyzed rocks are moderately potassic (K_2O = 2.94–3.40 wt.%). The content of K_2O reaches 4.14 wt.% in one sample (Table 1). The granites are characterized by high Al_2O_3 contents (from 15.8 to 16.8 wt.%).

On the diagram of B.R. Frost et al. (2001), the studied granites plot near the boundary between magnesian and ferroan rocks (FeO*/(FeO* + MgO) = 0.77–0.84) (Fig. 4*a*). In the classification by these authors, the Tutai granites are alkali-calcic (Fig. 4*b*) and weakly peraluminous (ASI = 0.99–1.14).

The Tutai granites show REE fractionation ($(La/Yb)_n$ = 11–35) and, mostly, a slight, if any, negative Eu anomaly (Eu/Eu* = 0.76–1.07) (Fig. 5*a*). A well-defined negative Eu anomaly is observed only for sample 11138 (Eu/Eu* = 0.56). The spidergrams show negative Th–U, Nb–Ta, P, and Ti anomalies and positive Ba and Sr anomalies (Fig. 5*b*). The Tutai granites are marked by low contents of Y (5–11 ppm) and Yb (0.51–0.81 ppm) and high contents of Sr (829–1529 ppm) and Ba (956–1391 ppm) (Table 1).

The South Ol'khon and Tutai granites are almost compositionally identical (Table 1, Fig. 3). They are characterized by high Al_2O_3 contents (16.00–16.15 wt.%), moderate K_2O contents (2.92–3.09 wt.%), and Na_2O/K_2O = 1.76–1.98. They plot within the same areas on the classification diagrams (Frost et al., 2001) as the Tutai granites (Fig. 4). The REE patterns and spidergrams are similar for the South Ol'khon and Tutai granites (Fig. 5).

In the South Ol'khon quartz syenites, SiO_2 = 61.5–62.9 wt.% and (Na_2O + K_2O) = 8.84–9.56 wt.% at Na_2O/K_2O = 0.91–1.76. They plot as quartz syenite and quartz monzonite on the diagram ($Na_2O + K_2O$)–SiO_2 (Middlemost, 1985) (Fig. 3). The ASI in the analyzed rocks is 0.89–0.93, suggesting that these rocks are metaluminous. On the diagrams of Frost et al. (2001), the quartz syenites plot near the boundaries between ferroan and magnesian as well as alkaline and alkali-calcic rocks (Fig. 4).

The quartz syenites are characterized by REE fractionation ($(La/Yb)_n$ = 5–22) and both positive and negative Eu anomalies (Eu/Eu* = 0.70–1.20) (Fig. 5*a*).

The quartz syenites have high contents of Sr (1542–1919 ppm) and Ba (1925–2981 ppm), somewhat higher than those in the Tutai and South Ol'khon granites. They have considerably higher contents of Y (25–38 ppm), Yb (2.09–3.54 ppm), and Nb (18.4–26.7 ppm) than the granites (Table 1). Despite increased alkali contents, the South Ol'khon quartz syenites are close to *I*- rather than *A*-type granites in the contents of trace and rare-earth elements. They do not plot as *A*-type granite (not shown) on the diagram FeO*/MgO–(Ce + Zr + Nb + Y) (Whalen et al., 1987).

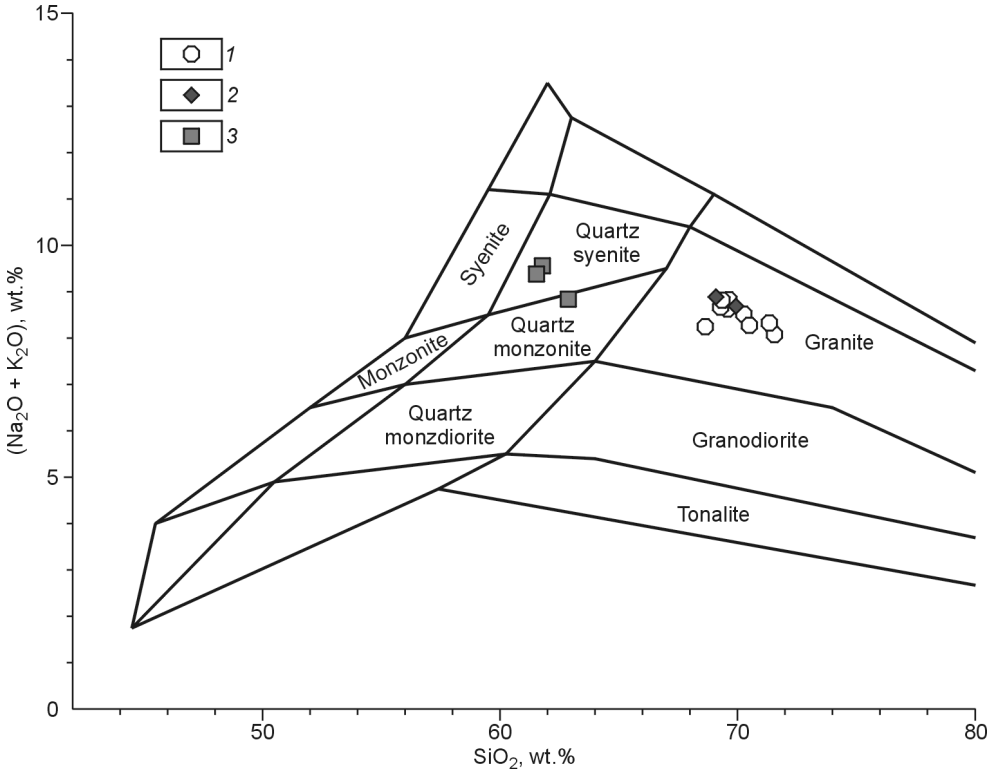

Fig. 3. Classification diagram ($Na_2O + K_2O$)–SiO_2 (Middlemost, 1985) for the Tutai and South Ol'khon granitoids. *1*, *2*, granites: *1*, Tutai; *2*, South Ol'khon; *3*, South Ol'khon syenites.

Table 1. Chemical composition of granitoids from the Tutai and South Ol'khon plutons

Component	Tutai pluton									South Ol'khon pluton[1]				
	1015	11135	11136	11137	11138	11139	11140	11141	11142	05140	05141	03239	03240	05145
	Granites									Granites		Quartz syenites		
SiO_2, wt.%	68.87	70.25	71.34	71.15	69.66	70.45	69.42	69.71	69.47	69.96	69.25	61.78	61.54	62.87
TiO_2	0.33	0.25	0.19	0.19	0.18	0.25	0.18	0.28	0.28	0.19	0.20	0.47	0.45	0.42
Al_2O_3	15.81	16.05	15.85	15.85	16.50	16.30	16.80	16.20	16.35	16.00	16.15	18.00	18.50	17.50
Fe_2O_3	0.94	0.81	0.83	0.53	0.44	0.59	0.93	0.73	1.00	–	–	–	–	–
FeO	1.85	1.43	1.11	1.48	1.46	1.36	1.17	1.52	1.17	–	–	–	–	–
Fe_2O_3*	–	–	–	–	–	–	–	–	–	2.19	2.15	3.75	4.08	3.85
MnO	0.04	0.03	0.04	0.03	0.02	0.03	0.05	0.03	0.03	0.04	0.04	0.09	0.09	0.10
MgO	0.82	0.49	0.40	0.36	0.41	0.53	0.48	0.45	0.51	0.49	0.51	1.06	0.94	1.22
CaO	2.44	1.53	1.41	1.35	1.62	1.50	2.02	1.63	1.67	1.93	2.25	3.77	3.92	3.93
Na_2O	5.17	5.45	4.96	4.83	4.34	5.04	5.25	5.33	5.43	5.44	5.78	4.56	4.99	5.64
K_2O	2.99	2.94	3.06	3.40	4.14	3.15	3.27	3.32	3.21	3.09	2.92	5.00	4.39	3.20
P_2O_5	0.13	0.09	0.08	0.06	0.10	0.09	0.10	0.10	0.17	0.07	0.07	0.23	0.22	0.22
H_2O^-	0.12	0.09	0.07	0.08	0.08	0.05	0.06	0.09	0.11	–	–	–	–	–
LOI	0.48	0.46	0.32	0.32	0.59	0.36	0.31	0.28	0.24	0.81	0.45	1.03	0.81	0.90
CO_2	n.d.	0.07	0.07	0.07	0.07	0.19	<0.06	<0.06	0.21	–	–	–	–	–
Total	99.99	99.94	99.73	99.70	99.61	99.89	100.04	99.67	99.85	100.21	99.77	99.74	99.93	99.85
Rb, ppm	38.1	37.2	45.0	54.4	88.1	43.9	41.6	36.4	34.7	34.9	32.2	68.5	54.9	41.7
Sr	1529	1353	1283	1084	829	1115	1450	1374	1294	1498	1552	1919	1821	1542
Y	9.2	10.9	6.5	5.7	8.6	5.1	10.4	5.6	6.3	13.6	20.9	25.1	38.2	33.4
Zr	147	145	186	120	118	112	131	131	125	122	142	162	114	150
Nb	12.9	5.7	3.1	5.5	5.6	4.0	4.0	4.4	5.1	10.3	11.2	26.3	26.7	18.4
Ba	1391	1189	1264	1144	956	1191	1238	1337	1252	1952	1665	2981	2896	1925
La	24.32	26.20	16.04	9.75	35.04	13.60	22.98	16.64	17.55	36.24	29.66	70.45	25.33	28.20
Ce	52.66	47.98	30.12	19.84	67.33	25.70	41.73	32.89	33.34	62.20	53.38	145.57	69.82	74.05
Pr	6.23	5.46	3.40	2.27	7.51	2.71	4.76	3.41	3.47	8.64	8.60	18.60	12.51	10.55
Nd	24.42	19.53	11.08	8.26	25.87	8.85	17.85	11.23	12.05	30.17	35.37	64.54	50.24	40.75
Sm	4.21	3.80	2.12	1.86	4.32	1.89	3.38	2.35	2.66	3.32	4.72	9.38	9.45	7.35
Eu	0.92	0.80	0.60	0.54	0.66	0.50	0.79	0.63	0.65	0.79	0.92	3.08	3.12	1.49
Gd	3.08	2.76	1.51	1.28	3.01	1.32	2.44	1.66	1.79	2.70	3.60	6.68	8.20	5.79
Tb	0.38	0.35	0.19	0.17	0.38	0.19	0.35	0.22	0.23	0.32	0.54	1.07	1.35	0.89
Dy	1.82	1.85	0.98	0.99	1.79	1.04	1.91	1.10	1.30	1.76	2.82	4.46	7.11	4.67
Ho	0.31	0.36	0.20	0.21	0.34	0.19	0.35	0.20	0.25	0.30	0.56	0.92	1.36	0.87
Er	0.87	0.97	0.52	0.60	0.82	0.51	0.89	0.53	0.64	1.16	1.81	2.53	4.64	2.90
Tm	0.13	0.13	0.08	0.10	0.11	0.08	0.13	0.08	0.09	0.18	0.28	0.43	0.37	0.53
Yb	0.81	0.79	0.47	0.61	0.66	0.52	0.77	0.51	0.56	0.53	1.07	2.17	3.54	2.09
Lu	0.14	0.12	0.08	0.11	0.11	0.09	0.13	0.09	0.09	0.14	0.24	0.36	0.41	0.38
Hf	3.19	3.40	4.21	3.09	3.11	3.10	2.94	2.97	2.94	2.65	3.14	3.68	2.33	3.13
Ta	0.53	0.19	0.09	0.27	0.16	0.17	0.20	0.15	0.21	0.49	0.77	1.61	2.42	1.27
Th	4.72	3.62	2.19	2.86	6.50	3.14	4.38	3.07	4.12	4.44	4.21	14.12	6.41	5.49
U	1.15	0.51	0.52	0.50	0.48	0.55	0.55	0.30	0.65	1.13	1.20	4.54	4.18	1.71
Na_2O/K_2O	1.73	1.85	1.62	1.42	1.05	1.60	1.61	1.61	1.69	1.76	1.98	0.91	1.14	1.76
FeO*/(FeO* + MgO)	0.77	0.82	0.82	0.84	0.82	0.78	0.81	0.83	0.80	0.80	0.79	0.76	0.80	0.74
ASI	0.99	1.08	1.14	1.13	1.14	1.14	1.07	1.07	1.07	1.02	0.97	0.92	0.93	0.89
$(La/Yb)_n$	20.0	22.1	22.6	10.7	35.4	17.3	19.9	22.0	20.9	45.7	18.5	21.7	4.8	9.0
Eu/Eu*	0.79	0.76	1.02	1.07	0.56	0.98	0.84	0.97	0.92	0.81	0.69	1.20	1.09	0.70
$Fe^{3+}/(Fe^{2+} + Fe^{3+})$	0.31	0.34	0.40	0.24	0.21	0.28	0.42	0.30	0.43	–	–	–	–	–
T, °C	764	775	804	766	764	759	764	764	760	754	760	751	724	742

Note. FeO* = FeO + 0.8998 · Fe_2O_3; Eu/Eu* = $Eu_n/\sqrt{(Sm_n \cdot Gd_n)}$; ASI(mol) = $Al_2O_3/(CaO - 1.67 \cdot P_2O_5 + Na_2O + K_2O)$; *n*, chondrite-normalized values (Nakamura, 1974); *T*, temperatures of early melt crystallization (zircon saturation temperatures) (Watson and Harrison, 1983). Dash, Not defined.

[1] The compositions of the South Ol'khon granites and quartz syenites are after (Gladkochub et al., 2008b).

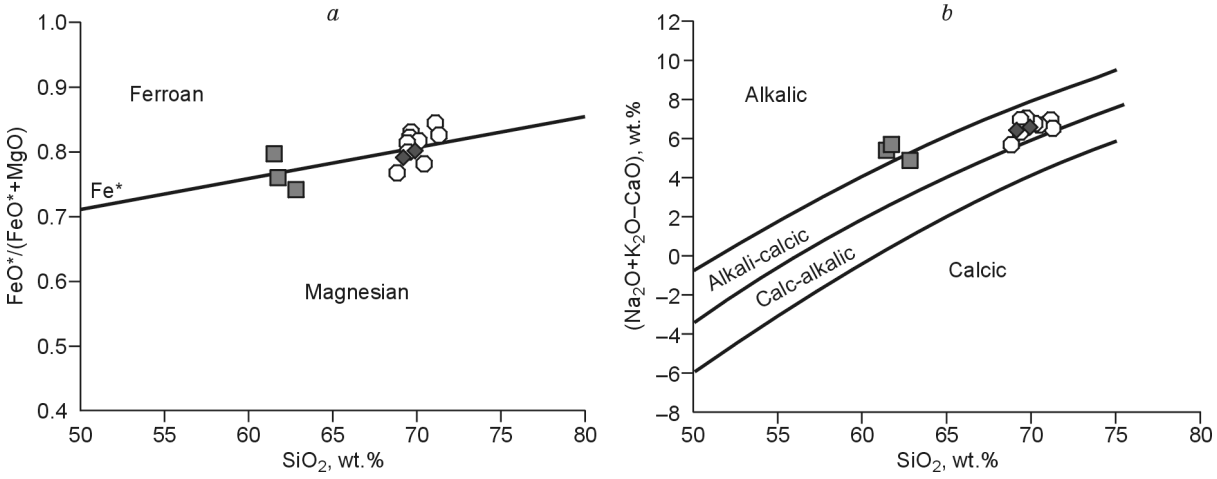

Fig. 4. Diagrams FeO*/(FeO* + MgO)–SiO_2 (*a*) and (Na_2O + K_2O – CaO)–SiO_2 (*b*) (Frost et al., 2001) for the Tutai and South Ol'khon granitoids.

U–Pb geochronological data

Sample 1015 was used in the dating of the Tutai granite (Fig. 2). Idiomorphic transparent and semitransparent light yellow and yellow crystals of accessory zircon were extracted from this sample. The grains are 200–300 μm in size, and the elongation index is 1:3. They show a distinct zoning on cathodoluminescence images (Fig. 6). The cores are characterized by a distinct magmatic zoning and $^{232}Th/^{238}U$ ratios of 0.12 to 0.62. The zircon rims show decreased luminescence and no zoning, with $^{232}Th/^{238}U$ ratios of 0.09–0.18. Note also the presence of highly luminescent fine rims in some zircon grains at the core–rim boundaries and on the crystal edges (Fig. 6). Eleven zircon grains were analyzed on a SHRIMP II, and the results are shown in Table 2 and Fig. 7. The mean weighted U–Pb age of the cores is 488.6 ± 8.0 Ma (MSWD = 3.9), and the mean weighted $^{206}Pb/^{238}U$ age of the rims is 464 ± 11 Ma (MSWD = 11.7). The age 488.6 ± 8.0 Ma, which is consistent with the morphology of the zircon grain cores (hence its magmatic origin), might be the most precise estimate of the crystallization age of zircon and, correspondingly, the age of the Tutai granites. The morphology of the zircon grain rims suggests its metamorphic origin, and the age 464 ± 11 Ma can be regarded as that of the metamorphic alterations of the Tutai granites.

Discussion

Formation conditions and sources of granitic melts

The presence of amphibole and titanite in the Tutai and South Ol'khon granites gives grounds for assigning them to the *I*-type in the "alphabetical" classification of granitoids (Chappell and White, 1974, 1992; Whalen et al., 1987). The assignment of these granites to the *I*-type is confirmed by moderate K_2O contents and high $Fe^{3+}/(Fe^{2+} + Fe^{3+})$ ratios (0.21–0.43 (Table 1) (Chappell and White, 1992). On the other hand, the weakly peraluminous composition (ASI = 0.97–1.14) and moderate CaO contents (Table 1) make them similar to *S*-type granites (Chappell and White, 1974, 1992). These mineral and geochemical characteristics permit assigning the Tutai and South Ol'khon granites to the transitional *I–S*-type (Liew et al., 1989) or *Ib*-type granites (Rosen and Fedorovskii, 2001). Most of the compositional points for the granites plot within the transitional *I–S* area on the ASI–SiO_2 diagram (Liew et al., 1989) (Fig. 8*a*). It is presumed that granitoids of such composition can be generated by the melting of mixed volcanosedimentary or metagraywacke sources and, probably, by the melting of lower-crust orthogneiss sources (Liew et al., 1989; Rosen and Fedorovskii, 2001). The composition of the source of the Tutai and South Ol'khon granites was estimated using the diagram Al_2O_3/(MgO + FeO*)–CaO/(MgO + FeO*) (Altherr et al., 2000), whose fields are delineated with regard to experimental data on the dehydration melting of rocks of different compositions. All the compositional points for the granites plot within the field of granitoids produced by the partial melting of metagraywacke protoliths (Fig. 8*b*).

The temperatures of the early crystallization of parental melts (more exactly, zircon saturation temperatures) were calculated using the thermometer of E.B. Watson and T.M. Harrison (1983). The calculation showed that the Tutai and South Ol'khon granites are characterized by moderate formation temperatures of 754–804 ºC (Table 1). These values correspond to so-called low-temperature granites of the *I*-type, whose hypothetical sources are quartz-feldspar crustal rocks (e.g., tonalitic gneisses) (Chappell et al., 1998). Chappell et al. (1998) pointed out that low-temperature granites of the *I*-type are similar to *S*-type granites, because the formation of both types of granites is accompanied by the melting of quartz-feldspar crust.

The most widespread rocks within the Anga–Satyurty megazone (Ol'khon terrane), which also contains the Pribrezhnaya zone with the Tutai and South Ol'khon granites, include the garnet-biotite gneisses in the amphibolitic facies and the garnet-orthopyroxene-biotite gneisses in the granulitic facies, which are geochemically similar to mature island-arc gray-

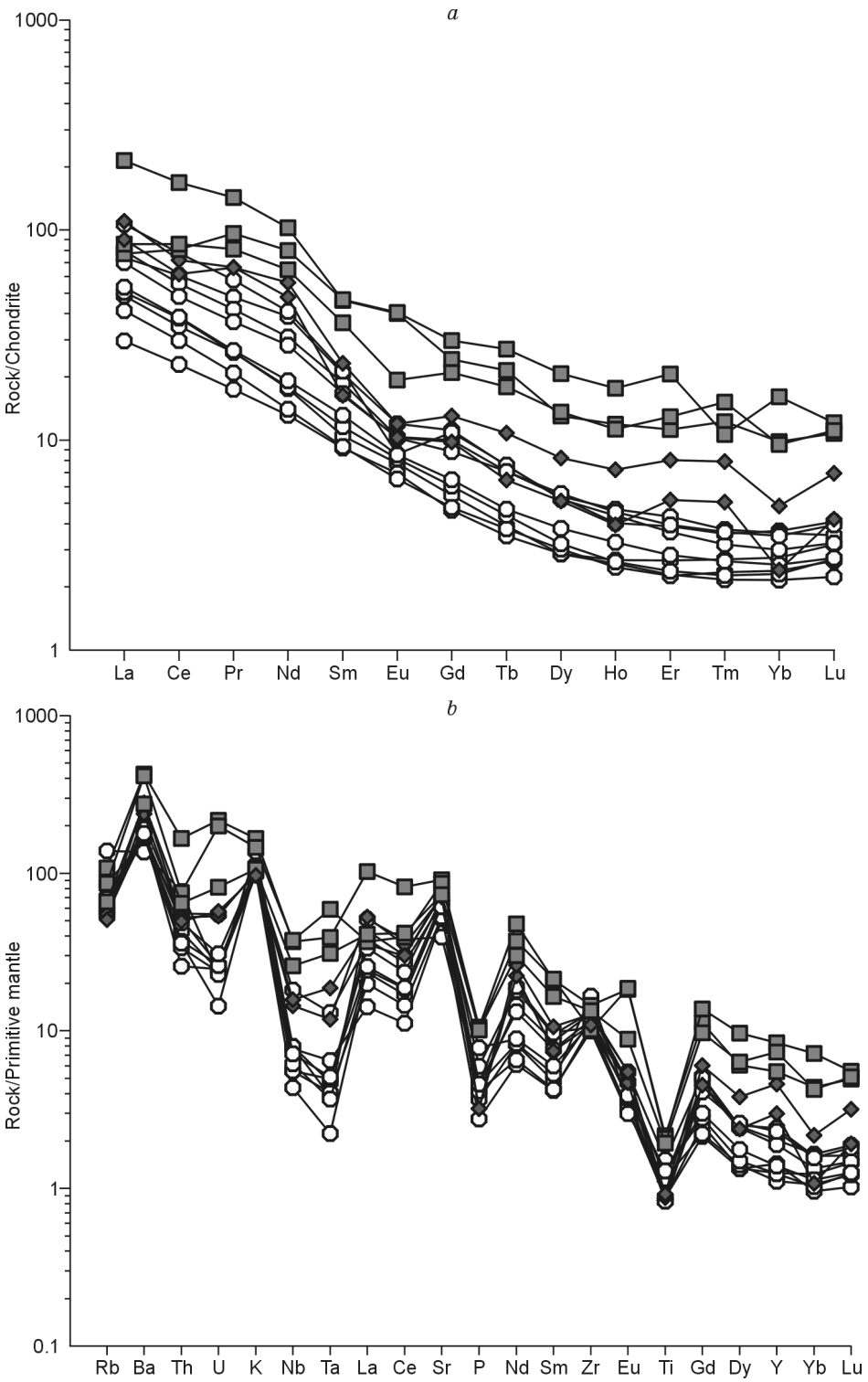

Fig. 5. Chondrite-normalized REE patterns (Nakamura, 1974) (*a*) and primitive mantle-normalized spidergrams (Sun and McDonough, 1989) (*b*) for the Tutai and South Ol'khon granitoids. See legend in Fig. 3.

wackes (Gladkochub et al., 2010; Makrygina et al., 2007). These metagraywackes have increased Al_2O_3 contents (>15 wt.%), low K_2O contents (1.1–2.3 wt.%), and high Ba contents (>500 ppm) ((Gladkochub et al., 2010; Makrygina et al., 2007) and the authors' unpublished data). In theory, the metagraywackes from the Anga–Satyurty megazone can be regarded as possible sources of the Tutai and South Ol'khon granites. However, since the host rocks of the granites are an alternation of sheets of different compositions, a different source (including a primary-magmatic one) is possible for these rocks. Anyway, quartz-feldspar crust is the possible protolith of the granites.

Table 2. U–Pb data on zircon from the Tutai granite (sample 1015)

Crystal, spot	Position	$^{206}Pb_c$, %	U	Th	$^{232}Th/^{238}U$	Isotopic ratios				Age, Ma		*D*, %
			ppm			$^{238}U/^{206}Pb^*$ (1)	±%	$^{207}Pb^*/^{206}Pb^*$ (1)	±%	$^{206}Pb/^{238}U$ (1)	$^{207}Pb/^{206}Pb$ (1)	
1.1	Core	0.25	985	590	0.62	12.6	0.6	0.0556	1.2	491 ± 3	437 ± 27	–13
2.1	Core	0.11	1180	201	0.18	12.9	0.6	0.0559	0.9	481 ± 3	450 ± 21	–7
3.1	Rim	0.08	771	74	0.10	13.3	0.7	0.0548	1.1	467 ± 3	405 ± 26	–16
4.1	Rim	0.07	731	86	0.12	13.5	0.8	0.0573	1.3	460 ± 3	503 ± 29	+9
5.1	Core	0.12	955	111	0.12	12.7	11.1	0.0554	1.1	490 ± 52	429 ± 23	–15
6.1	Core	0.10	719	324	0.47	12.4	0.7	0.0566	1.1	498 ± 4	474 ± 25	–5
7.1	Rim	0.10	490	56	0.12	13.2	0.7	0.0560	1.4	472 ± 3	453 ± 31	–4
7.2	Core	0.16	448	174	0.40	12.7	0.7	0.0580	1.8	488 ± 3	530 ± 39	+8
8.1	Rim	0.16	895	79	0.09	13.1	0.6	0.0555	1.2	475 ± 3	433 ± 27	–10
9.1	Rim	0.08	805	142	0.18	13.6	0.7	0.0564	1.4	457 ± 3	468 ± 31	+2
10.1	Rim	0.09	584	76	0.13	13.9	0.7	0.0565	1.3	449 ± 3	470 ± 29	+5
11.1	Core	0.42	808	444	0.57	13.5	3.4	0.0561	1.6	460 ± 15	458 ± 35	0

Note. The error is within a 1σ interval. Pb_c and Pb*, Common and radiogenic Pb, respectively. *D*, Discordance.
(1) corrected for common Pb using ^{204}Pb.

The low Y and Yb contents of the Tutai and South Ol'khon granites (Table 1) suggest the presence of garnet among the restite phases (Patiño Douce and Beard, 1996; Turkina, 2000). The slight or absent Eu anomaly on the REE patterns for almost all the granites (except sample 11138) (Fig. 5*a*), along with the high Sr contents of the samples (>1000 ppm), suggests the absence of plagioclase among the restite phases. According to (Patiño Douce and Beard, 1996), the melting of metagraywacke and orthogneiss (tonalitic) protoliths under garnet crystallization follows a similar scenario: Incongruent melting, accompanied by plagioclase disintegration and albite release, increases the Na_2O content of the melt and, correspondingly, the Na_2O/K_2O ratios. High Na_2O contents and $Na_2O/K_2O > 1$ are the distinguishing features of the Tutai and South Ol'khon granites (Table 1). This permits such a scenario of granite formation regardless of the protolith (metagraywacke or orthogneiss). Deep crustal melting is important for the generation of felsic magmas in the case of garnet crystallization in restite and, correspondingly, at moderate or high pressures. This presupposes crustal thickening before the start of melting (Patiño Douce and Beard, 1996).

Unlike the Tutai and South Ol'khon granites, the South Ol'khon quartz syenites have decreased SiO_2 contents (61.5–62.9 wt.%), suggesting their generation not only from metagraywacke or orthogneiss protoliths. The quartz syenites are metaluminous rocks with ASI < 1 (Table 1). On the diagram

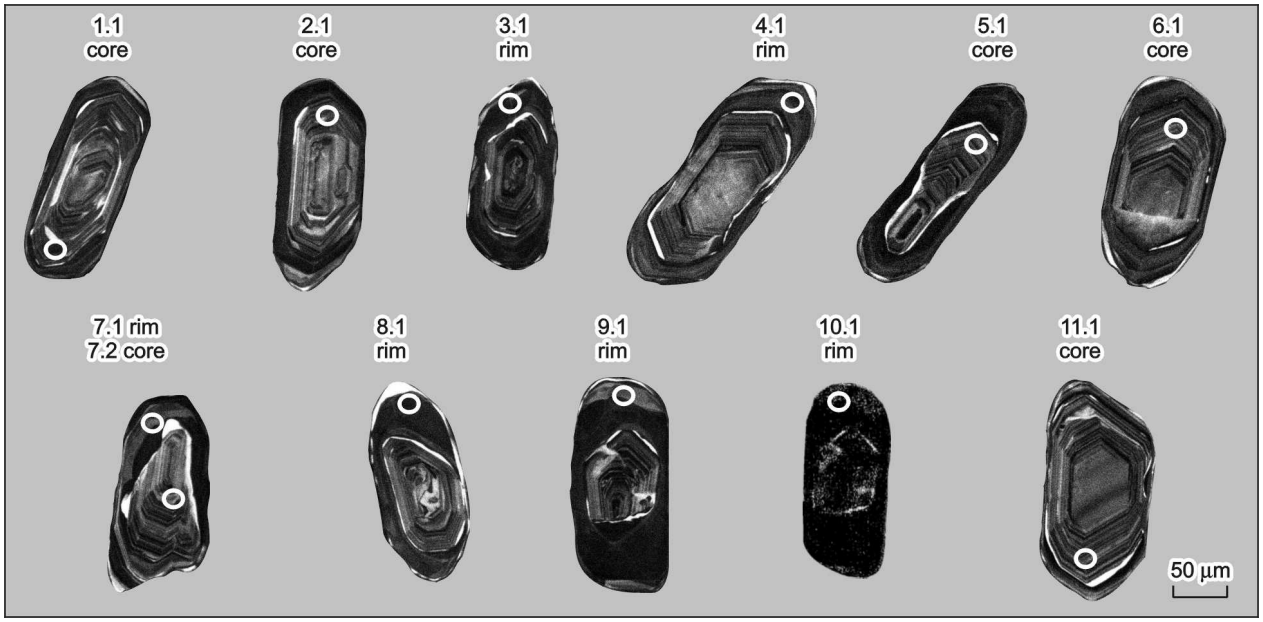

Fig. 6. Cathodoluminescence images of zircon crystals from the Tutai granite, sample 1015.

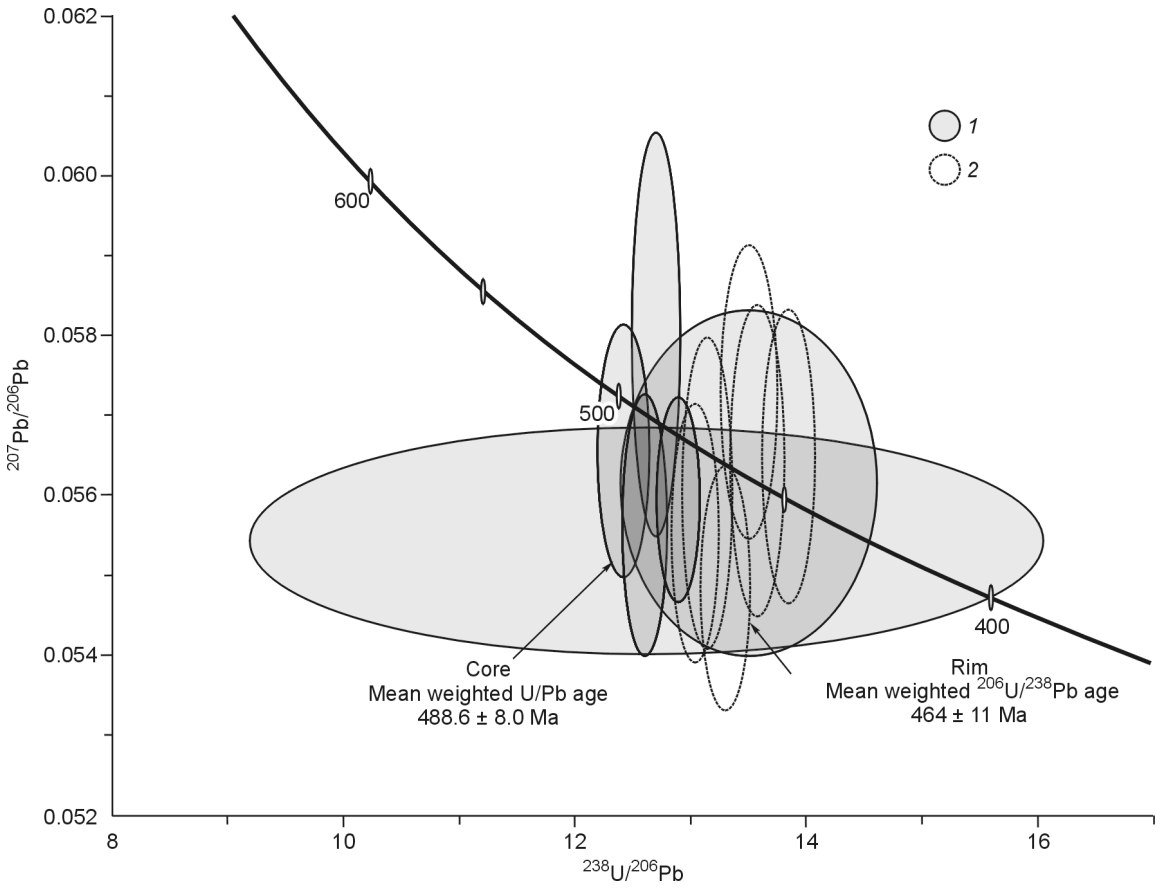

Fig. 7. $^{207}Pb/^{206}Pb$–$^{238}U/^{206}Pb$ diagram (Tera and Wasserburg, 1972) for zircon from the Tutai granite (sample 1015). *1*, core; *2*, rim.

$Al_2O_3/(MgO + FeO^*)$–$CaO/(MgO + FeO^*)$, they plot as rocks produced by the melting of metamafic/metatonalitic sources (Fig. 8*b*). The high Y and Yb contents of the quartz syenites (Table 1) indicate a disequilibrium with garnetiferous parageneses during the formation and evolution of the quartz syenite magmas. The calculated zircon saturation temperatures (Watson and Harrison, 1983) for the quartz syenites are quite low (724–751 ºC), even lower than those in the granites (Table 1). Apparently, these values are underestimated, because the quartz syenites have low Zr contents (114–162 ppm), suggesting that the Zr content of the melt was not enough for zircon saturation. Besides that, the quartz syenites show high cation ratios (M[1] = 1.90–1.95), which also complicate the use of the thermometer (Watson and Harrison, 1983) to estimate the crystallization temperatures of the quartz syenites, because this geothermometer is reliable for rocks with M values from 0.9 to 1.7. However, the magnesian composition of some analyzed varieties of quartz syenites (Fig. 4*a*) and the moderate contents of elements such as Zr, Nb, and Y permit a comparison between the studied rocks and *I*-type (not *A*-type) granites, suggesting their moderate melting temperatures.

The Nd isotope composition of the quartz syenites ($\varepsilon_{Nd}(T)$ = –0.3 (Gladkochub et al., 2008b)) is less radiogenic than that of the mantle rocks in the Anga–Satyurty megazone (both metamorphic and the youngest, unaltered rocks) with $\varepsilon_{Nd}(T)$ = +2.4 to +3.7 ((Gladkochub et al., 2008b) and the authors' unpublished data) but significantly more radiogenic than in the metaterrigenous rocks of this zone ($\varepsilon_{Nd}(T)$ = –3.2 to –25.8 (Gladkochub et al., 2008b; Vladimirov et al., 2008)). Thus, the South Ol'khon quartz syenites are, most likely, of crust-mantle origin. The geochemical features of the quartz syenites are very high Ba and Sr contents (Table 1), which might reflect the trace-element characteristics of the mantle protolith (Tarney and Jones, 1994; Turkina, 2005). On the other hand, the well-defined Nb–Ta, P, and Ti anomalies on the spidergrams (Fig. 5*b*) suggest the presence of crust in the quartz syenite source. The combined isotopic and geochemical data suggest the formation of the South Ol'khon quartz syenites as a result of crust–mantle interaction. The absence of any signs of equilibrium between the quartz syenite magmas and garnetiferous restite and/or cumulus associations suggests that crustal and mantle magmas mixed in the middle crust above the depth at which the Tutai and South Ol'khon granites were generated (lower crust, garnet stability field in restite).

Since the almost simultaneous formation and evolution of the melts of the Tutai and South Ol'khon granites and quartz syenites took place at different *PT*-parameters and different

[1] $M = (Na + K + 2 \cdot Ca)/(Al \cdot Si)$, where Na, K, Ca, Al, and Si are the contents of elements in rock (Watson and Harrison, 1983).

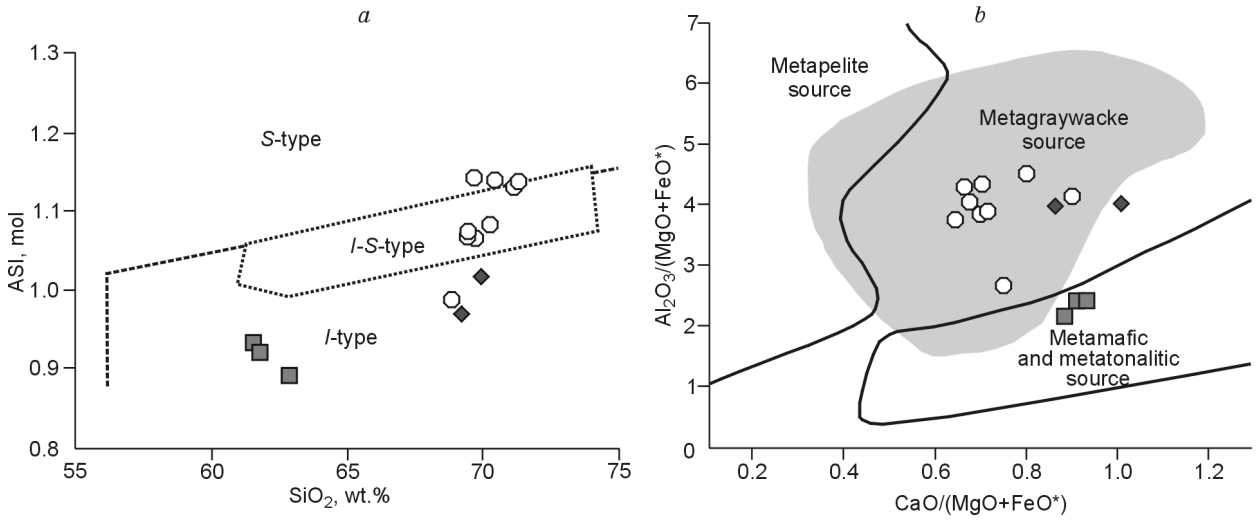

Fig. 8. ASI–SiO_2 (Liew et al., 1989) (*a*) and Al_2O_3/(MgO + FeO*)–CaO/(MgO + FeO*) (Altherr et al., 2000) (*b*) diagrams for the Tutai and South Ol'khon granitoids. ASI(mol) = $Al_2O_3/(CaO - 1.67\ P_2O_5 + Na_2O + K_2O)$. See legend in Fig. 3.

crustal depths, a necessary condition for their generation is the existence of thickened crust. The additional heat source, which caused melting under ongoing folding in the region, might have been the underplating of basaltic melts to the base of thickened crust. The underplating was only a heat source for the granites, whereas for the quartz syenites, these basaltic melts can be regarded as a possible supplier of mantle matter to the area of magma generation.

Scenario of the geodynamic evolution of the eastern Ol'khon terrane

Before try to decipher the scenario of the geodynamic evolution of the eastern Anga–Satyurty megazone (Ol'khon terrane) and the entire megazone, let us summarize the main conclusions from the study of the Tutai and South Ol'khon granitoids.

(1) The intrusion of the granitoids during the second deformation stage and the formation of F_2 folds permit regarding the studied granitoid plutons not only as synfolding but also as synmetamorphic. It is also evident that the granitoids and host rocks were later affected by synmetamorphic deformations D_3 and D_4. We emphasize that no signs of discreteness (breaks, stops) were observed in the deformation process or metamorphism;

(2) The Tutai granites were dated by the U–Pb zircon method at 488.6 ± 8.0 Ma. The coincidence within error between the previous age estimate for the South Ol'khon quartz syenites (495 ± 6 Ma (Gladkochub et al., 2008b)) and the age of the Tutai granites suggests that the rocks of these plutons are of close ages, almost coeval. On the other hand, structural data suggest that the given geochronological determinations also correspond to the age of early metamorphism and deformations. Later metamorphism and deformations took place at 464 ± 11 Ma (estimated age of the rims of zircon grains from the Tutai granites), and the entire history of the granites and quartz syenites, as well as that of deformations and metamorphism, is limited to this time interval;

(3) The geochemical characteristics of the Tutai and South Ol'khon granites indicate that their formation took place in the lower crust (area of garnet stability in restite) and the quartz syenites might have formed in the middle crust, because the quartz syenite magmas bear no signs of equilibrium with garnetiferous restite and/or cumulus parageneses. A quartz-feldspar crustal protolith (metagraywacke or orthogneiss) is determined for the Tutai and South Ol'khon granites, whereas a mixed (crust-mantle) source is presumed for the South Ol'khon quartz syenites. A necessary condition for the formation of the Tutai and South Ol'khon rocks was protolith melting within thickened crust.

Original data on the Tutai and South Ol'khon granitoids, combined with published data on the geology, tectonics, and age of the rocks within the Ol'khon terrane (Bibikova et al., 1990; Fedorovsky et al., 2005, 2010; Gladkochub et al., 2008b; and others), suggest a scenario of the geodynamic evolution of the eastern Anga–Satyurty megazone (Ol'khon terrane) and probably the entire Anga–Satyurty megazone.

The intrusion of the granitoids during the second deformation stage in the region and their formation within thickened crust suggest that the moment of the granitoid formation was preceded by tectonic events, which created conditions favorable to the granitoid formation. We presume that the crustal thickening was due to the accretion of some tectonic units which consist of rocks of different compositions (fragments of different parts of a backarc (marginal) basin (Gladkochub et al., 2008b; Makrygina et al., 2007; Zorin et al., 2009)) in the present-day eastern Ol'khon terrane. This stage is reflected in the presence of F_1 and F_2 folds in the Pribrezhnaya zone rocks. On the other hand, regional structural observations suggest that these early accretion events were much more widespread, affecting the entire Anga–Satyurty megazone, which includes the Pribrezhnaya zone. Early sheet-type folds with gentle hinges occur widely in the area, and their

formation was always followed by total synmetamorphic shearing, which created the collisional collage of the present-day area. Examples include the sheet fold stacks preserved among the shear structures of the Nutgei zone, numerous relict areas of such structures in the southwestern Chernorud zone, direct evidence for early sheet deformations within the Main shear zone, etc. All this suggests that an important accretion stage should be distinguished in the region. It occurs widely, up to the oblique collision of all the fragments of the accreted tectonosphere and the Siberian craton.

Apparently, the accretionary structure formed above the subduction zone. The identification and direction of this zone remain disputable (Gladkochub et al., 2008b; Zorin et al., 2009), and we do not discuss this problem in the paper. Models for the formation of accretionary orogens above the subduction zone assume that the formation of the orogen created conditions for crustal thickening and more intense shortening, which favored the tectonic clustering of rock complexes, shearing, and thrusting (Collins, 2002; Zorin et al., 2009). During the same period, the underplating of basaltic melts to the crustal base caused granulite-facies metamorphism and initiated granitoid melting (Collins, 2002). Extending the above-mentioned regularities in the evolution of accretionary orogens to the Anga–Satyurty megazone, we presume that the granulites, now observed in the Chernorud zone of the Ol'khon area and in northern Ol'khon Island, might have been formed at the base of such an accreted structure. The time of early accretion in this case corresponds to the age of the granulites and equals 507–498 Ma (Gladkochub et al., 2008b). The basaltic magmas which intruded the crustal base might have served not only as the initiators of granulite-facies metamorphism but also as a necessary heat source for the melting of the Tutai and South Ol'khon granitoids. As was pointed out above, the Tutai and South Ol'khon granites were produced by the melting of the quartz-feldspar protolith in the lower crust, whereas the South Ol'khon quartz syenites formed owing to crust–mantle interaction in the middle crust. The granitoid intrusion itself took place during tectonic events in the region, more specifically, during the second deformation stage (with the formation of F_2 folds), which suggests ongoing compression. Also, the 485–494 Ma synmetamorphic hypersthene granites (Bibikova et al., 1990; Khromykh, 2006), observed among the Chernorud zone granulites and structurally related to the early sheet folds, might be the indicators of these events.

The compression in the Pribrezhnaya zone and the entire region did not end at that stage, because the granitoids and the host rocks were later affected by deformations D_3 and D_4. The time of these events can be estimated from the age of the metamorphic rims in the Tutai granites, which equals 464 ± 11 Ma. For the entire Ol'khon terrane, this event might reflect convergence with the Siberian craton, the end of accretion, and giant oblique collision of all the components of the system. During the collision and attendant strike-slip tectonics, the initial system was destroyed and its components were dismembered and mixed owing to sliding along the cratonic edge. These events reflect the available age estimates for different manifestations of magmatism at 458–470 Ma. The strike-slip tectonics also determined the start of the synorogenic collapse of the collisional structure. This complicated collisional collage with extant elements of accretionary geodynamics is observed in the present-day Ol'khon region.

We thank N.N. Kruk and S.N. Rudnev for constructive comments, which helped us to improve the paper.

The study was supported by the Russian Foundation for Basic Research (grants no. 12-05-00749 and 11-05-00267) and the Siberian Branch of the Russian Academy of Sciences (partner project of basic research no. 79).

References

Altherr, R., Holl, A., Hegner, E., Langer, C., Kreuzer, H., 2000. High-potassium, calc-alkaline I-type plutonism in the European Variscides: northern Vosges (France) and northern Schwarzwald (Germany). Lithos 50 (1–3), 51–73.

Bibikova, E.V., Karpenko, S.F., Sumin, L.V., Bogdanovskii, O.G., Kirnozova, T.I., Lyalikov, A.V., Makarov, V.A., Arakelyants, M.M., Korikovskii, S.P., Fedorovskii, V.S., Petrova, Z.I., Levitskii, V.I., 1990. U–Pb, Sm–Nd, Pb–Pb, and K–Ar ages of metamorphic and igneous rocks from the Ol'khon region (western Cisbaikalia), in: Shemyakin, V.M. (Ed.), Precambrian Geology and Geochronology of the Siberian Platform and Its Framing [in Russian]. Nauka, Leningrad, pp. 170–183.

Chappell, B.W., White, A.J.R., 1974. Two contrasting granite types. Pacific Geol. 8, 173–174.

Chappell, B.W., White, A.J.R., 1992. I- and S-type granites in the Lachlan Fold Belt. Trans. R. Soc. Edinburgh: Earth Sci. 83, 1–26.

Chappell, B.W., Bryant, C.J., Wyborn, D., White, A.J.R., Williams, I.S., 1998. High- and low-temperature I-type granites. Res. Geol. 48 (4), 225–235.

Collins, W.J., 2002. Hot orogens, tectonic switching, and creation of continental crust. Geology 30 (6), 535–538.

Dobretsov, N.L., Buslov, M.M., 2007. Late Cambrian-Ordovician tectonics and geodynamics of Central Asia. Russian Geology and Geophysics (Geologiya i Geofizika) 48 (1), 71–82 (93–108).

Donskaya, T.V., Sklyarov, E.V., Gladkochub, D.P., Mazukabzov, A.M., Sal'nikova, E.B., Kovach, V.P., Yakovleva, S.Z., Berezhnaya, N.G., 2000. The Baikal collisional metamorphic belt. Dokl. Earth Sci. 374 (7), 1075–1079.

Fedorovskii, V.S., Vladimirov, A.G., Khain, E.V., Kargapolov, S.A., Gibsher, A.S., Izokh, A.E., 1995. Tectonics, metamorphism, and magmatism in Caledonide collisional zones of Central Asia. Geotektonika, No. 3, 3–22.

Fedorovskii, V.S., Sklyarov, E.V., Mazukabzov, A.M., Gladkochub, D.P., Donskaya, T.V., Izokh, A.E., Lavrenchuk, A.V., Agatova, A.R., Kotov, A.B., 2011. Aerospace Geological Map of the Northeastern Ol'khon Region (Baikal). Nutgei and Orgoita–Zmeinaya Creek Zones. Ol'khon Geodynamic Site, Scale 1 : 20,000 [in Russian]. A1 TIS, Moscow.

Fedorovsky, V.S., Donskaya, T.V., Gladkochub, D.P., Khromykh, S.V., Mazukabzov, A.M., Mekhonoshin, A.S., Sklyarov, E.V., Sukhorukov, V.P., Vladimirov, A.G., Volkova, N.I., Yudin, D.S., 2005. The Ol'khon collision system (Baikal region), in: Sklyarov, E.V. (Ed.), Structural and Tectonic Correlation across the Central Asia Orogenic Collage: North-Eastern Segment, Guidebook and Abstract Volume of the Siberian Workshop IGCP-480. Print. IEC SB RAS, Irkutsk, pp. 5–76.

Fedorovsky, V.S., Sklyarov, E.V., Izokh, A.E., Kotov, A.B., Lavrenchuk, A.V., Mazukabzov, A.M., 2010. Strike-slip tectonics and subalkaline mafic magmatism in the Early Paleozoic collisional system of the western Baikal region. Russian Geology and Geophysics (Geologiya i Geofizika) 51 (5), 534–547 (682–700).

Frost, B.R., Barnes, C.G., Collins, W.J., Arculus, R.J., Ellis, D.J., Frost, C.D., 2001. A geochemical classification for granitic rocks. J. Petrol. 42 (11), 2033–2048.

Garbe-Schönberg, C.-D., 1993. Simultaneous determination of thirty-seven trace elements in twenty-eight international rock standards by ICP-MS. Geostand. Newslett. 17 (1), 81–97.

Gladkochub, D.P., Donskaya, T.V., Fedorovsky, V.S., Mazukabzov, A.M., Wingate, M.T.D., Poller, U., Todt, W., 2008a. New data on the age and protolith of granulites of the Olkhon collisional system (Baikal Region). Dokl. Earth Sci. 419A (3), 417–422.

Gladkochub, D.P., Donskaya, T.V., Wingate, M.T.D., Poller, U., Kröner, A., Fedorovsky, V.S., Mazukabzov, A.M., Todt, W., Pisarevsky, S.A., 2008b. Petrology, geochronology, and tectonic implications of c. 500 Ma metamorphic and igneous rocks along the northern margin of the Central Asian Orogen (Olkhon terrane, Lake Baikal, Siberia). J. Geol. Soc. London 165 (1), 235–246.

Gladkochub, D.P., Donskaya, T.V., Fedorovsky, V.S., Mazukabzov, A.M., Larionov, A.N., Sergeev, S.A., 2010. The Olkhon metamorphic terrane in the Baikal region: An Early Paleozoic collage of Neoproterozoic active margin fragments. Russian Geology and Geophysics (Geologiya i Geofizika) 51 (5), 447–460 (571–588).

Khromykh, S.V., 2006. Igneous Petrology of Deep Levels of the Collisional System (as Illustrated by Early Caledonides in the Ol'khon Region of Western Cisbaikalia). Extended Abstract of Cand. Sci. (Geol.–Mineral.) Dissertation. Inst. Geol. Mineral., Novosibirsk.

Kuklei, L.N., 1988. Tectonic Structures of Granitization (Western Cisbaikalia) [in Russian]. Nauka, Moscow.

Liew, T.C., Finger, F., Höck, V., 1989. The Moldanubian granitoid plutons of Austria: Chemical and isotopic studies bearing on their environmental setting. Chem. Geol. 76 (1–2), 41–55.

Ludwig, K.R., 2008. User's Manual for Isoplot 3.6: A Geochronological Toolkit for Microsoft Excel. Berkeley Geochronology Center Spec. Publ. 4, Berkeley.

Ludwig, K.R., 2009. User's Manual for SQUID 2. Berkeley Geochronology Center Spec. Publ. 5, Berkeley.

Makrygina, V.A., Belichenko, V.G., Reznitsky, L.Z., 2007. Types of paleoisland arcs and back-arc basins in the northeast of the Paleoasian Ocean (from geochemical data). Russian Geology and Geophysics (Geologiya i Geofizika) 48 (1), 107–119 (141–155).

Mazukabzov, A.M., Donskaya, T.V., Gladkochub, D.P., Paderin, I.P., 2010. The Late Paleozoic geodynamics of the West Transbaikalian segment of the Central Asian fold belt. Russian Geology and Geophysics (Geologiya i Geofizika) 51 (5), 482–491 (615–628).

Metelkin, D.V., Vernikovsky, V.A., Kazansky, A.Yu., 2012. Tectonic evolution of the Siberian paleocontinent from the Neoproterozoic to the Late Mesozoic: paleomagnetic record and reconstructions. Russian Geology and Geophysics (Geologiya i Geofizika) 53 (7), 675–688 (883–899).

Middlemost, E.A.K., 1985. Magmas and Magmatic Rocks: An Introduction to Igneous Petrology. Longman, Essex.

Nakamura, N., 1974. Determination of REE, Ba, Fe, Mg, Na and K in carbonaceous and ordinary chondrites. Geochim. Cosmochim. Acta 38 (5), 757–775.

Nozhkin, A.D., Bayanova, T.B., Turkina, O.M., Travin, A.V., Dmitrieva, N.V., 2005. Early Paleozoic granitoid magmatism and metamorphism on the Derba microcontinent, eastern Sayan region: New isotope–geochronological data. Dokl. Earth Sci. 404 (7), 1084–1089.

Paces, J.B., Miller, J.D., Jr., 1993. Precise U-Pb ages of Duluth Complex and related mafic intrusions, northeastern Minnesota: Geochronological insights to physical, petrogenic, paleomagnetic, and tectonomagmatic processes associated with the 1.1 Ga Midcontinent Rift System. J. Geophys. Res. B: Solid Earth 98 (B8), 13,997–14,013.

Panteeva, S.V., Gladkochoub, D.P., Donskaya, T.V., Markova, V.V., Sandimirova, G.P., 2003. Determination of 24 trace elements in felsic rocks by inductively coupled plasma mass spectrometry after lithium metaborate fusion. Spectrochim. Acta, Part B, 58 (2), 341–350.

Patiño Douce, A.E., Beard, J.S., 1996. Effects of P, $f(O_2)$ and Mg/Fe ratio on dehydration melting of model metagreywackes. J. Petrol. 37 (5), 999–1024.

Rosen, O.M., Fedorovskii, V.S., 2001. Collisional Granitoids and Crustal Delamination (Examples of Cenozoic, Paleozoic, and Proterozoic Collisional Systems) [in Russian]. Nauchnyi Mir, Moscow.

Rytsk, E.Yu., Kovach, V.P., Makeev, A.F., Bogomolov, E.S., Rizvanova, N.G., 2009. The eastern boundary of the Baikal collisional belt: Geological, geochronological, and Nd isotopic evidence. Geotektonika, No. 4, 16–26.

Salnikova, E.B., Sergeev, S.A., Kotov, A.B., Yakovleva, S.Z., Steiger, R.H., Reznitskiy, L.Z., Vasil'ev, E.P., 1998. U-Pb zircon dating of granulite metamorphism in the Sludyanskiy complex, Eastern Siberia. Gondwana Res. 1 (2), 195–205.

Sklyarov, E.V., Fedorovsky, V.S., Kotov, A.B., Lavrenchuk, A.V., Mazukabzov, A.M., Levitsky, V.I., Sal'nikova, E.B., Starikova, A.E., Yakovleva, S.Z., Anisimova, I.V., Fedoseenko, A.M., 2009. Carbonatites in collisional settings and pseudo-carbonatites of the Early Paleozoic Ol'khon collisional system. Russian Geology and Geophysics (Geologiya i Geofizika) 50 (12), 1091–1106 (1409–1427).

Sukhorukov, V.P., Travin, A.V., Fedorovsky, V.S., Yudin, D.S., 2005. The age of shear deformations in the Ol'khon region, western Cisbaikalia (from results of $^{40}Ar/^{39}Ar$ dating). Russian Geology and Geophysics (Geologiya i Geofizika) 46 (5), 567–571 (579–583).

Sun, S.-s., McDonough, W.F., 1989. Chemical and isotopic systematics of oceanic basalts: implications for mantle composition and processes, in: Saunders, A.D., Norry, M.J. (Eds.), Magmatism in the Oceanic Basins. Geol. Soc. London. Spec. Publ. 42 (1), 313–345.

Tarney, J., Jones, C.E., 1994. Trace element geochemistry of orogenic igneous rocks and crustal growth models. J. Geol. Soc. London 151 (5), 855–868.

Tera, F., Wasserburg, G.J., 1972. U-Th-Pb systematics in lunar highland samples from the Luna 20 and Apollo 16 missions. Earth Planet. Sci. Lett. 17 (1), 36–51.

Turkina, O.M., 2000. Modeling geochemical types of tonalite–trondhjemite melts and their natural equivalents. Geochem. Int. 38 (7), 640–651.

Turkina, O.M., 2005. Proterozoic tonalites and trondhjemites of the southwestern margin of the Siberian craton: isotope geochemical evidence for the lower crustal sources and conditions of melt formation in collisional settings. Petrology 13 (1), 35–48.

Turner, F.J., Weiss, L.E., 1963. Structural Analysis of Metamorphic Tectonites. McGraw-Hill, New York.

Vladimirov, A.G., Khromykh, S.V., Mekhonoshin, A.S., Volkova, N.I., Travin, A.V., Yudin, D.S., Kruk, N.N., 2008. U–Pb dating and Sm–Nd systematics of igneous rocks in the Ol'khon region (Western Baikal Coast). Dokl. Earth Sci. 423A (9), 1372–1375.

Vladimirov, A.G., Volkova, N.I., Mekhonoshin, A.S., Travin, A.V., Vladimirov, V.G., Khromykh, S.V., Yudin, D.S., Kolotilina, T.B., 2011. The geodynamic model of formation of Early Caledonides in the Olkhon Region (West Pribaikalie). Dokl. Earth Sci. 436 (2), 203–209.

Volkova, N.I., Sklyarov, E.V., 2007. High-pressure complexes of Central Asian Fold Belt: geologic setting, geochemistry, and geodynamic implications. Russian Geology and Geophysics (Geologiya i Geofizika) 48 (1), 83–90 (109–119).

Volkova, N.I., Vladimirov, A.G., Travin, A.V., Mekhonoshin, A.S., Khromykh, S.V., Yudin, D.S., Rudnev, S.N., 2010. U–Pb isotopic dating of zircons (SHRIMP-II) from granulites of the Ol'khon region of Western Baikal area. Dokl. Earth Sci. 432 (2), 821–824.

Watson, E.B., Harrison, T.M., 1983. Zircon saturation revisited: temperature and composition effects in a variety of crustal magma types. Earth Planet. Sci. Lett. 64 (2), 295–304.

Whalen, J.B., Currie, K.L., Chappell, B.W., 1987. A-type granites: geochemical characteristics, discrimination and petrogenesis. Contrib. Mineral. Petrol. 95 (4), 407–419.

Williams, I.S., 1998. U-Th-Pb geochronology by ion microprobe, in: McKibben, M.A., Shanks, W.C. III, Ridley, W.I. (Eds.), Applications of Microanalytical Techniques to Understanding Mineralizing Processes. Rev. Econ. Geol. 7, 1–35.

Zorin, Yu.A., Sklyarov, E.V., Belichenko, V.G., Mazukabzov, A.M., 2009. Island arc–back-arc basin evolution: implications for Late Riphean–Early Paleozoic geodynamic history of the Sayan–Baikal folded area. Russian Geology and Geophysics (Geologiya i Geofizika) 50 (3), 149–161 (209–226).